Physica Medica 114 (2023) 103136

Contents lists available at ScienceDirect

Physica Medica

journal homepage: www.elsevier.com/locate/ejmp

Evaluation of a novel phantom for the quality assurance of a six-degree-of-freedom couch 3D-printed at multiple centres

Hannah Marshall [a,*], Tamil Selvan [b], Reem Ahmad [c], Mariana Bento [c], Catarina Veiga [c], Gordon Sands [d], Ciaran Malone [e], Raymond B King [b], Catharine H Clark [c,d,f], Conor K McGarry [a,b]

[a] Patrick G. Johnston Centre for Cancer Research, Queen's University Belfast, Belfast, UK
[b] Department of Radiotherapy Physics, Northern Ireland Cancer Centre, Belfast Health and Social Care Trust, Belfast, UK
[c] Department of Medical Physics and Biomedical Engineering, University College London, London, UK
[d] Radiotherapy Physics, UCLH NHS Foundation Trust, London, UK
[e] Radiotherapy Physics, St. Luke's Radiation Oncology Network, Dublin, Ireland
[f] Metrology for Medical Physics, National Physical Laboratory, Teddington, UK

ARTICLE INFO

Keywords:
6DoF
3D-printing
Six-degrees-of-freedom
Quality assurance

ABSTRACT

This study aimed to validate a bespoke 3D-printed phantom for use in quality assurance (QA) of a 6 degrees-of-freedom (6DoF) treatment couch. A novel phantom design comprising a main body with internal cube structures, was fabricated at five centres using Polylactic Acid (PLA) material, with an additional phantom produced incorporating a PLA-stone hybrid material. Correctional setup shifts were determined using image registration by 3D-3D matching of high HU cube structures between obtained cone-beam computer tomography (CBCT) images to reference CTs, containing cubes with fabricated rotational offsets of 3.5°, 1.5° and −2.5° in rotation, pitch, and roll, respectively. Average rotational setup shifts were obtained for each phantom. The reproducibility of 3D-printing was probed by comparing the internal cube size as well as Hounsfield Units between each of the uniquely produced phantoms. For the five PLA phantoms, the average rot, pitch and roll correctional differences from the fabricated offsets were $-0.3 \pm 0.2°$, $-0.2 \pm 0.5°$ and $0.2 \pm 0.3°$ respectively, and for the PLA hybrid these differences were $-0.09 \pm 0.14°$, $0.30 \pm 0.00°$ and $0.03 \pm 0.10°$. There was found to be no statistically significant difference in average cube size between the five PLA printed phantoms, with the significant difference ($P < 0.05$) in HU of one phantom compared to the others attributed to setup choice and material density. This work demonstrated the capability producing a novel 3D-printed 6DoF couch QA phantom design, at multiple centres, with each unique model capable of sub-degree couch correction.

1. Introduction

Modern radiation therapy (RT) linear accelerators utilise precise robotic positioning couches, to move the patient into a desired position for treatment. Conventionally, these couches were limited to only four degrees of freedom (4DoF), in the form of translational motion in the lateral, longitudinal and vertical directions as well as yaw rotation. Couches capable of six degrees of freedom provide the traditional couch motions with the addition of pitch and roll rotations. 6DoF couches have the potential to provide more accurate, and consistent inter-fractional, patient positioning which is a crucial component in ensuring the conformal delivery of large radiation doses with high precision [1]. Consequently, tolerance limits for couches with rotational correction capabilities are advised in Task Group (TG) 142 and Medical Physics Practice Guideline 8a [2,3] by the American Association of Physicists in Medicine (AAPM), to be 1 mm/0.5° in translational and rotational movement, respectively, for stereotactic treatments. Quality assurance (QA) is crucial in ensuring consistent couch performance, however, research studies focused on the development and evaluation of QA systems for 6DoF couches are limited [4–8,11–12].

3-Dimensional (3D) printing, also termed additive manufacturing (AM), is emerging as a promising technique to produce phantoms for radiotherapy applications, with the number of publications in this area increasing year-on-year [9,10]. Fused deposition modelling (FDM) is a 3D printing technique by which melted thermoplastics are extruded layer-by-layer into a specified shape. FDM allows for custom geometries

* Corresponding author.
E-mail address: hannah.marshall@belfasttrust.hscni.net (H. Marshall).

https://doi.org/10.1016/j.ejmp.2023.103136
Received 3 April 2023; Received in revised form 18 August 2023; Accepted 13 September 2023
Available online 26 September 2023

to be printed for little expense relative to that associated with the purchase of commercial RT phantoms, due to the inexpensive nature of commonly used printing materials. A study by Woods et al. [11] demonstrated the feasibility of implementing 3D printed phantoms into the QA of 6DoF couches, with daily registration data obtained over a 30-day period, for three phantoms, achieving uncertainties within the recommended AAPM tolerances for both translational and rotational motions. However, the main limitation of this study was variation in designed offset dimensions of the three phantoms, which was of millimetre magnitude despite the printer being specified to have sub-millimetre accuracy. Further work by Popreeda et al proposed a method of semi-automated 6DoF couch QA using a 3D-printed phantom and both image displacement and an accelerometer sensor. However, the accelerometer sensor was not used for yaw rotation due to dimensional inaccuracy [12]. To fully evaluate the feasibility of using 3D-printed phantoms in quality assurance, multi-centre investigations are crucial to probe reproducibility when varying printer and material specifications.

This study aimed to design, fabricate, and validate a 3D-printed phantom to be used for the routine QA of 6DoF couches, with a specific focus on the correction of rotational couch motions through daily validation. Additionally, this work aims to demonstrate the feasibility of producing and distributing STL files to allow for multi-centre 6DoF couch audits. This study also aimed to investigate the reproducibility of additive manufacturing in producing QA phantoms, through the verification of phantoms printed at five centres, utilising various 3D printers and thermoplastic manufacturers. To the best of our knowledge this work is the first time that 3D printing has been used in a multi-centre study to fabricate a phantom for 6DoF couch QA.

2. Materials and methodology

2.1. Phantom design

A virtual phantom designed using the ImSimQA^{TM} (Oncology Systems Limited, Shrewsbury UK) software was adapted for this project. Reference synthetic CT images of the phantom, with slice thickness of 1 mm, were created within ImSimQA^{TM} for the purpose of image registration with applied rotations in rotation (rot), pitch and roll directions of 3.5°, 1.5° and −2.5° respectively, applied to each of the internal cube structures, relative to the phantom body. These rotation values, which are notably large rotations compared to common clinically used values, were selected to both ensure that shift from initial position was easily observed, and to assess the couch performance towards the limits of their range. The initial design was fabricated with three internal cubes (Fig. 1a), each with a complex internal structure, as shown in Fig. 1b and Fig. 1c, to assist with 3D-3D registration. The body of the phantom was designed to be 150 mm in each dimension (Fig. 1a), with exterior recessed markings with zero rotation and extruding crosshairs, of height 3 mm, with rotations equal to those of the internal structures in the synthetic CT. A hollowed recess, measuring 35 mm in width and 5 mm in depth, containing two protruding cylinders, diameter 10 mm, along the bottom of the phantom allowed the base to be securely attached to a lock bar, ensuring reproducible couch set-up (Fig. 1f).

2.2. 3-Dimensional printing

The virtual phantom was exported from ImSimQA^{TM} as a stereolithography (STL) file and manipulated by a slicing software to generate GCODE, which contains instructions to be interpreted by the printer. Both files were distributed to the collaborating centres (Table 1), alongside the recommended print settings described in this section. Four out of the five centres used the STL file (including the centre distributing the files), one centre opted to alter the GCODE file due to difficulties slicing the file appropriately using the STL in their selected software. The infill density, which defines the ratio of printed plastic to air in a specified region, was set to 40% rectilinear with a line width of 50% for the phantom body, such that the line infill structure was not resolved by the CT scanner (Fig. 2c-d). The cube structures were assigned 100% rectilinear infill with a line width of 100%, where it should be noted that

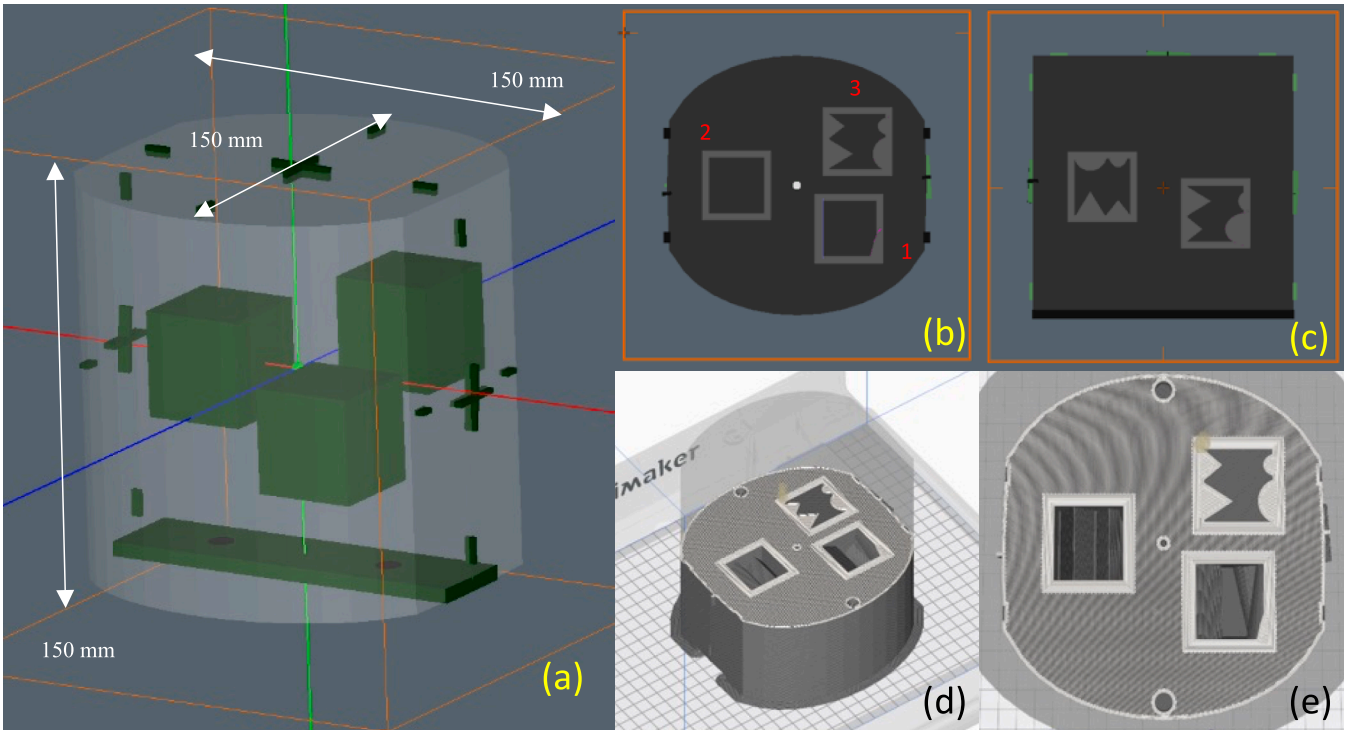

Fig. 1. (a) Phantom structure in ImSimQA^{TM}, dimensions of phantom exterior are given· (b) and (c) synthetic CT images generated in ImSimQA^{TM}, prior to rotations being applied to cube structures. (d) and (e) Lower half of phantom body in Ultimaker Cura^{TM} slicer software, preparing for print.

Table 1
Table describing the 3D printer, slicer software and manufacturer of printing filament used by each of the centres in this study. Each phantom is given a number, which it will be referred by throughout this work, with the PLA-hybrid phantom denoted by 6*. Mass density values given from product specifications supplied by each manufacturer.

Phantom	Centre	3D-Printer	Slicer Software	Filament Manufacturer	Filament Mass Density (gcm^{-3})
1	University College London (UCL) Department of Medial Physics and Biomedical Engineering	Raise3D Pro+	Simplify3D Version 4.1.2	Raise3D (Premium) PLA	1.2
2	University College London (UCL) Department of Medial Physics and Biomedical Engineering	Ultimaker S5	Cura Version 4.8.0	Ultimaker PLA	1.24
3	University College London Hospitals (UCLH) NHS Foundation Trust	Raise3D Pro+	IdeaMaker Version 4.2.1	3D Fuel Standard PLA Polylite PLA	1.24 1.17–1.24
4	St Luke's Radiation Oncology Network (SLRON) Dublin	Airwolf Axiom 20	Apex Version 1.3.9	RS Pro PLA	1.24
5	Northern Ireland Cancer Centre (NICC)	Ultimaker S5	Cura Version 4.6.2	RS Pro PLA	1.24
6*	Northern Ireland Cancer Centre (NICC)	Ultimaker S5	Cura Version 4.6.2	RS Pro PLA FormFutura StoneFil™ (cube structures) *	1.24 1.70*

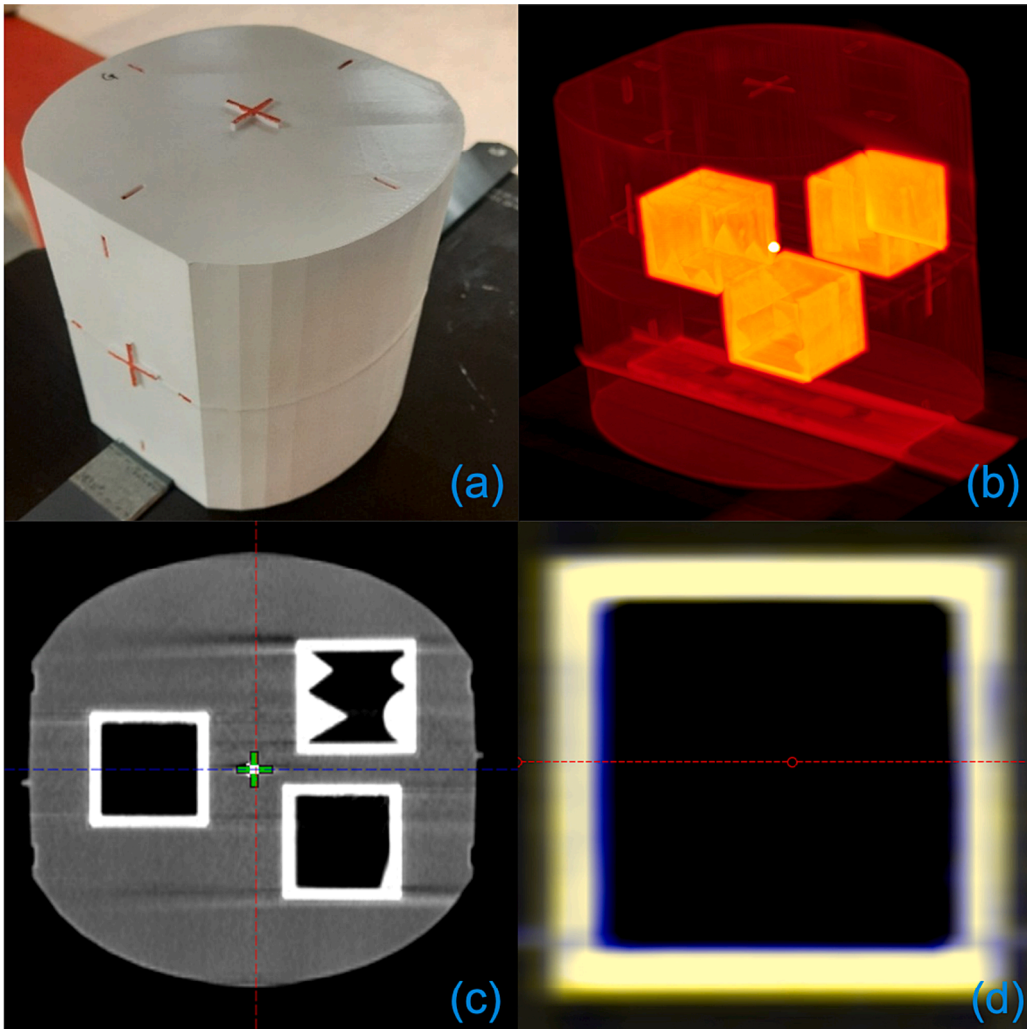

Fig. 2. (a) Complete 3D-printed phantom, fully assembled, attached to lock bar. (b-c) CT images obtained of the phantom, demonstrating the complex features of the internal cube structures in each dimension, used for 3D-3D matching. (d) Registration of PLA and PLA-hybrid phantoms, with line profile across cube region to determine HU.

the central region of each cube is hollow, as shown in Fig. 1. Higher infill density of the cube structures allows greater CT contrast from the phantom body, for the purpose of registration (Fig. 2c-d). Five phantoms were printed with PLA filament across five centres, each with varying combinations of 3D printer and PLA, summarised in Table 1. Each phantom was printed as two separate halves, with an average printing time across centres of 3.5 days for each half. Two cylindrical alignment plugs, for which a separate STL file was distributed, were printed separately to the main body of the phantom, using 40% rectilinear infill and 50% infill line width. The plugs were inserted into cylindrical hollows on the inner surface of the phantom, to ensure the secure attachment of the two halves. A central recess allowed for a 1/8″ ball bearing to

be placed in the centre of the phantom before sealing the two halves together. Fig. 2a shows the exterior of a fully assembled 6DoF phantom, with Fig. 2b demonstrating the location of the internal structures.

It should be noted that whilst a list of recommended settings was distributed to each centre, there are many settings which may be altered in 3D-printing which can impact the geometrical and radiological properties of the finished product. Some commonly altered settings, such as retraction and flow rate, were left to be defined by each centre to achieve the best quality print for their specific printer and material manufacturer. A post-print questionnaire completed by each centre identified values used for some of the commonly altered print settings which may impact print quality, these details can be found in the supplementary material.

An additional, sixth phantom was produced to probe the effect of varying material on CT contrast. For this phantom, the main body was printed using PLA, however, the cube structures were printed separately with a PLA-hybrid material containing powdered stone, StoneFil^{TM} (FormFutura, Nijmegen the Netherlands). Previous literature [12–14] has demonstrated the capability of StoneFil^{TM} in achieving Hounsfield Units (HU) comparable with that of bone structures, with up to 800 HU achievable dependent on flow rate print setting. This material was therefore selected for the purpose of image registration using high HU. The method of production for this additional phantom was different to the other phantoms produced in this study, with the cubes being printed independently of the main body, which was similarly printed in two halves.

2.3. Rotational couch correction

The Northern Ireland Cancer Centre has ten linear accelerators (linacs), three of which are equipped with 6-degree-of-freedom couches. One of these machines, defined locally as linear accelerator 8 (LA8) was used to obtain rotational couch corrections on a daily basis, for a period of 2 years, using phantom 6*. The phantom was firmly attached to the PerfectPitch 6DoF couch of LA8, a Varian TrueBeam STx v.2.5 (Varian Medical Systems, Palo Alto, CA, USA), by attaching the protruding cylinders to a lock bar. The couch was shifted such that the recessed markings on the phantom exterior were in alignment with the lasers in the room. Kilo-voltage cone beam computed tomography (kV-CBCT) was performed on the treatment console using locally defined 'head SRS' exposure parameters (full fan, bowtie filter, 100 kVp, 100 mAs, 1 mm slice thickness). A 3D-3D auto-match registration was performed, at the linac, between the reconstructed image and the synthetic reference CT, with fabricated cube offsets.

Translational shifts were first confirmed to be within a locally defined tolerance of 2 mm, rotational shifts were recorded and applied to the couch. Positional verification was performed by observing alignment of the lasers with the extruding crosshairs on the phantom exterior, for which the rotational offset is equal to that of the cube structures in the synthetic CT. The positional accuracy of the extruding crosshairs was independently validated by comparing shifts observed in moving from the centre of the setup markers to the centre of the crosshairs on both the synthetic CT and when manually moving the treatment couch to alter the phantom position. Additionally, for phantom 6* only, monthly verification of rotational correction was performed on the couch using a digital inclinometer on graph paper to measure variation from couch positions 0° to ±3°, in 1° increments for roll and pitch, as recommended in IPEM report 81 [15]. The reproducibility between phantoms was probed by performing the method of positional verification described above, repeated 5 times to produce average values, for phantoms 1–5. One-way analysis of variance (ANOVA) testing was performed to probe any variations in rotational corrections, in all three dimensions, between each of the phantoms produced in this study. ANOVA was also used to probe any difference between the rotational corrections for phantoms 1–5 and phantom 6*, due to the different method of fabrication.

A synthetic CT, whereby the internal cube structures were free from rotations, was produced to probe, through CT-synthetic CT registration, the actual offsets of the cubes which may differ from the design due to variations in 3D printing. The offsets measured were used to correct the measured rotational corrections obtained for each phantom from 6DoF couch registration, to negate the impact of initial cube offset as a result of 3D-printing.

2.4. Geometrical measurements

CT images were obtained for each of the phantoms produced for this study, using a Siemens (Munich, Germany) SOMATOM CT scanner at 120kVp peak tube potential and a slice thickness of 2 mm. Average HU for PLA were calculated using regions of interest which encapsulated each cube structure. These were defined by image thresholding with a range of 0 to 900 HU which generated contours for each of the cubes in a reproducible, non-subjective manner, whilst negating any contribution from the air gaps inside the cube structures. HU profiles were generated through the centre of each of the cubes, in the three cardinal planes, to determine the dimensions of the cubes. Due to the partial volume effect and the limited resolution of the CT images, the outline of the cubes were inherently blurred. Therefore, the cube edges were not clearly defined on the images, the point where the HU value fell to half its maximum was assumed as a suitable surrogate. The full width half-maximum HU was therefore determined, for both peaks in the profile, by taking the average of the minimum and maximum HU values of the peak. The size value corresponding to half-maximum HU was then determined using the FORECAST function in Microsoft Excel (Microsoft Corporation, Redmond, Washington). Total cube size was calculated as the difference between the two size values from each peak in the profile. This process was repeated for each dimension, for each cube in each of the phantoms produced in this study, allowing average HU and cube size to be determined. One-way analysis of variance (ANOVA) testing was performed to probe differences in average cube size between each of the five PLA phantoms and additionally between the phantoms where the cube structures were printed with PLA and the phantom where cubes were printed with StoneFil^{TM}. Further ANOVA testing was performed to probe differences in average HU obtained, across all three cubes, from the five PLA phantoms and additionally to probe any difference in HU between cube structures within each phantom produced.

3. Results

3.1. 6DoF registration

Rotational couch corrections were recorded daily, over a period of 2 years for phantom 6*. For the period of measurement, the rot, pitch and roll measurements were found to vary by no more than ± 0.3° (Fig. 3) from the designed offset values of 3.5°, 1.5° and −2.5°, respectively. Within a 95% confidence interval, with 2 standard deviations (2σ), the rot, pitch and roll measurements over the 2-years of measurement were found to be on average 3.5 ± 0.2°, 1.7 ± 0.1° and −2.5 ± 0.1°. Considering the fabricated offset values, these measurements gave on average correctional differences of −0.1 ± 0.2°, 0.2 ± 0.1° and 0.0 ± 0.1° which were within AAPM recommended rotational tolerance of 0.5°. If the first 3 months of rotational couch corrections were averaged and considered as baseline values for phantom 6*, on this couch, the average correctional differences from these baseline values over the remaining recorded period are −0.2°, 0.0° and 0.1° in rot, pitch, and roll, respectively. Additional monthly verification of rotational correction of the three rotational DoF showed differences from the designed offsets of ± 0.1° and ± 0.2° for roll and pitch, respectively, with all but one measurement for rotational correction within ± 0.3°.

For all six phantoms, an average of the rot, pitch and roll corrections over five measurements was determined (Fig. 4). The average rot, pitch and roll measurements across phantoms 1–5 were found to be 3.3 ±

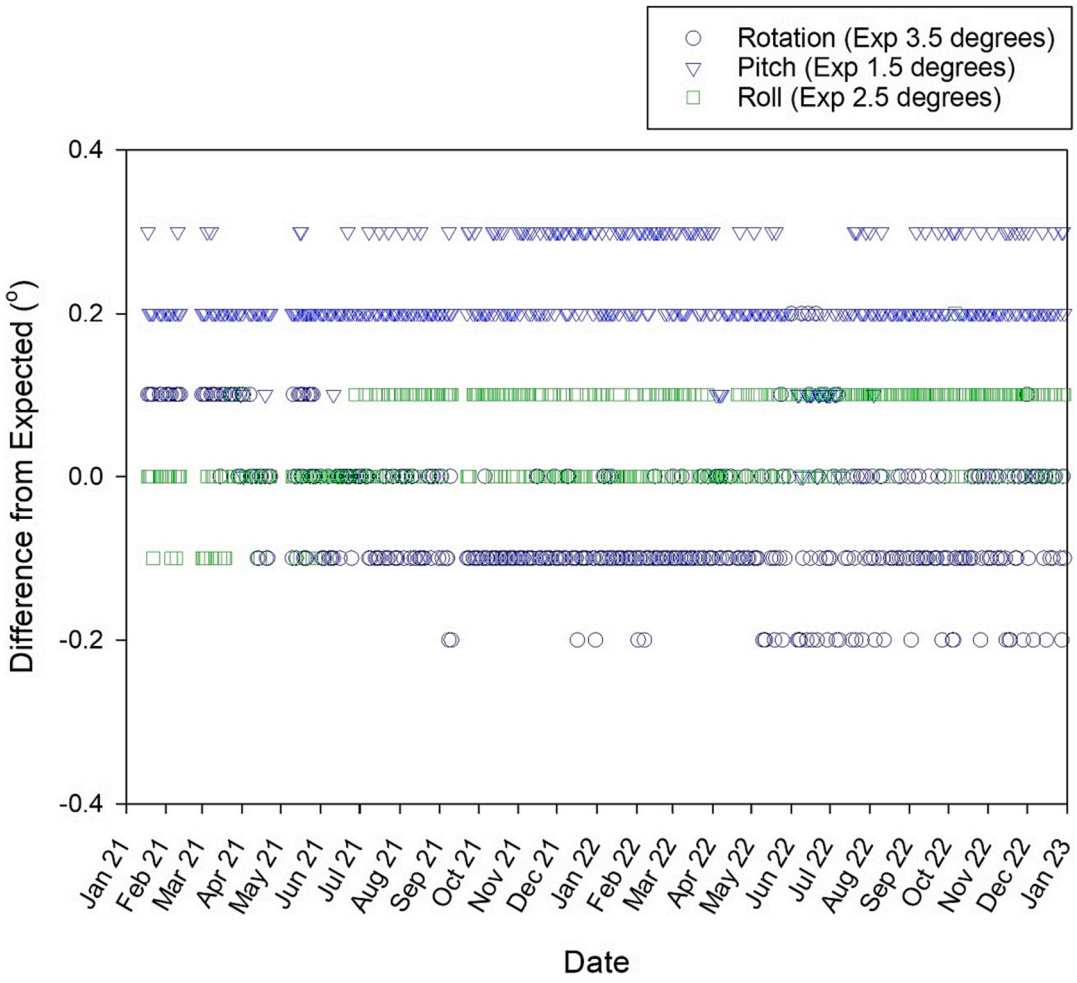

Fig. 3. Difference from expected fabricated rotational offsets for the PLA Hybrid Phantom over a period of 2 years. Legend identifies each of the rotational corrections and their corresponding expected value.

0.2°, 1.3 ± 0.5° and −2.3 ± 0.3°, respectively, with 2σ uncertainty. These results for phantom 6* were 3.4 ± 0.1°, 1.8 ± 0.0° and −2.5 ± 0.1°, respectively. It was found however, that there are statistically significant differences in all three rotational degrees between the average values determined for phantoms 1–5 ($p < 0.05$). Additionally, there was found to be statistically significant differences in the average rot, pitch and roll measurements between each of the phantoms 1–5 and phantom 6*.

By registering the CT images of each phantom with a rotation-free synthetic CT, the 'actual' cube offsets were determined. The results of the rotational corrections were corrected by the 'actual' offsets to account for variation that may be induced due to 3D printing, this gave rise to an average rotational correction of 3.2 ± 0.2°, 1.4 ± 0.2° and −2.4 ± 0.1° for phantoms 1–5 and 3.2 ± 0.1°, 1.8 ± 0.0° and −2.5 ± 0.0° for phantom 6* in rot, pitch and roll, respectively. Fig. 5 shows the average rotational shifts for each phantom, when corrected for the 'actual' cube offsets measured. It was found that whilst statistically significant differences ($p < 0.05$) still occurred between phantoms 1–5 and between phantoms 1–5 and 6* for rot and pitch, post-correction by 'actual' cube offsets, there was found to be no statistically significant difference between phantoms 1–5 and between phantoms 1–5 and 6* in roll. Additionally, when corrected for 'actual' cube offsets, it was found that all rotational corrections measured for phantom 6* over two years were within ± 0.2°, in all three rotational dimensions, from the fabricated values.

3.2. Geometrical measurements

The average size of each of the three internal cube structures was determined for each of the six phantoms. These results (Fig. 6) demonstrate that geometrical variations occur, despite five phantoms all being printed with PLA. It was found that there was no statistically significant difference in the average cube size between phantoms 1–5. However, the average cube size of phantom 6* showed a statistically significant difference from phantoms 1–5 ($p < 0.05$), which were printed with only PLA using a different method of fabrication. In all six of the phantoms produced for this study, there was no statistically significant difference in the average size of each of the three cubes. The cube structures printed using phantom 6* were found to be closer to the specified cube size of 4.0 cm in each dimension, with an average cube size of 4.0 ± 0.1 cm. Cubes printed with standard PLA, had an average size across phantoms 1–5 of 4.2 ± 0.0 cm. The correlation between the difference of cube sizes and differences in corresponding rotational corrections was investigated, with no statistically significant correlation between the two variables found.

3.3. Hounsfield Units

Hounsfield units were determined for the internal cube structures over a region of interest spanning the length of the cube. The average HU for all three cubes, for each of the six phantoms is shown in Fig. 7, where the expected average HU for PLA and StoneFil are indicated in this figure. There was a statistically significant difference in the average HU

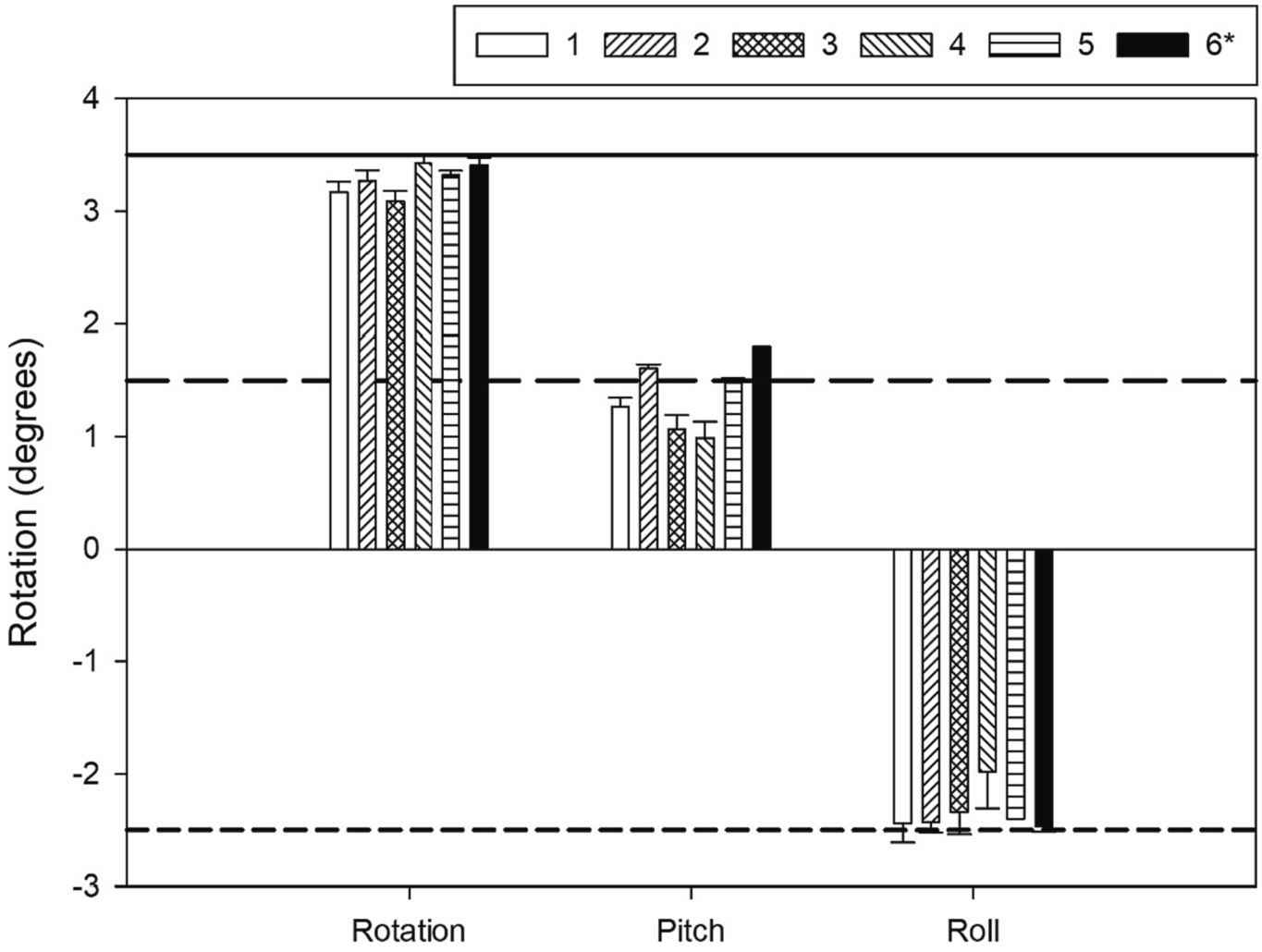

Fig. 4. Average rotational shifts across 5 measurements, for each phantom. Legend identifies centre and printer, as per Table 1, where * represents the additional PLA hybrid phantom produced by the NICC. Designed fabricated offset values of 3.5°, 1.5° and −2.5° in rotation, pitch and roll are given by the black solid, medium-dashed, and fine- dashed lines respectively.

between phantoms 1–5 ($p < 0.05$). Further investigations found that these differences arose from phantom 1 with an average HU of 139 ± 6, with there being no statistically significant difference between the average HU of phantoms 2–5. There was a statistically significant difference in average HU achieved between each of the phantoms 1–5 and 6* ($p < 0.05$), which was expected due to the higher density of the StoneFil^{TM} material. The HU achieved by printing with standard PLA filament was on average 190 ± 30 (where the error is one standard deviation), when averaging across all 3 cubes and phantoms 1–5. However, if considering only the four phantoms with no statistically significant difference in average HU, this mean value becomes 197 ± 3. The cube structures printed using StoneFil^{TM} (phantom 6*) allowed for higher average HU of 480 ± 20 to be achieved. The correlation between the differences in HU and differences in rotational corrections was investigated, with no statistically significant correlation between the two variables found.

4. Discussion

A novel 3D-printed phantom was designed and utilised to verify sub-degree rotational corrections of a 6-degree-of-freedom treatment couch. The registration of six independently produced phantoms verified that rotational differences were within the AAPM recommended tolerance of 0.5° [2–3], allowing the implementation of this phantom design into daily couch QA. Over a period of 2 years, daily use of this phantom design did not give rise to any rotational corrections outside of the recommended AAPM tolerance of 0.5°. Intercomparison between phantoms produced at different centres demonstrated the reproducibility of 3D printing, to produce 6DoF phantoms with sub-degree accuracy.

Rotational corrections for phantom 6* were recorded as part of daily QA of a 6DoF couch, for a period of 2 years. During this period, the differences between the observed correction and the fabricated rotational offsets did not exceed the AAPM recommended tolerance of 0.5°, with average values of −0.1 ± 0.2°, 0.2 ± 0.1° and 0.0 ± 0.1° in rot, pitch, and roll, respectively. These results are in-line with those of Popreeda et al [12], where couch position errors measured using an image displacement method were found to be 0.20°,0.07° and 0.23° rot, pitch and roll, respectively. A study completed by Woods et al [11], observed the registration values for three 3D-printed phantoms across 3 linacs for a period of 30 days. The three phantoms were fabricated with offset capability of 2.0°, −2.0° and 2.0° in pitch, roll and rot, respectively, and registration values with 2σ uncertainty were reported to be 2.0 ± 0.4°, −2.4 ± 0.3° and 2.0 ± 0.4° when combining the results across the three linacs in each rotational dimension. Whilst the uncertainty in the daily rotational corrections reported by Woods et al are larger than those reported in this study, this may be a result of combining data for three independent phantoms, each registered on a

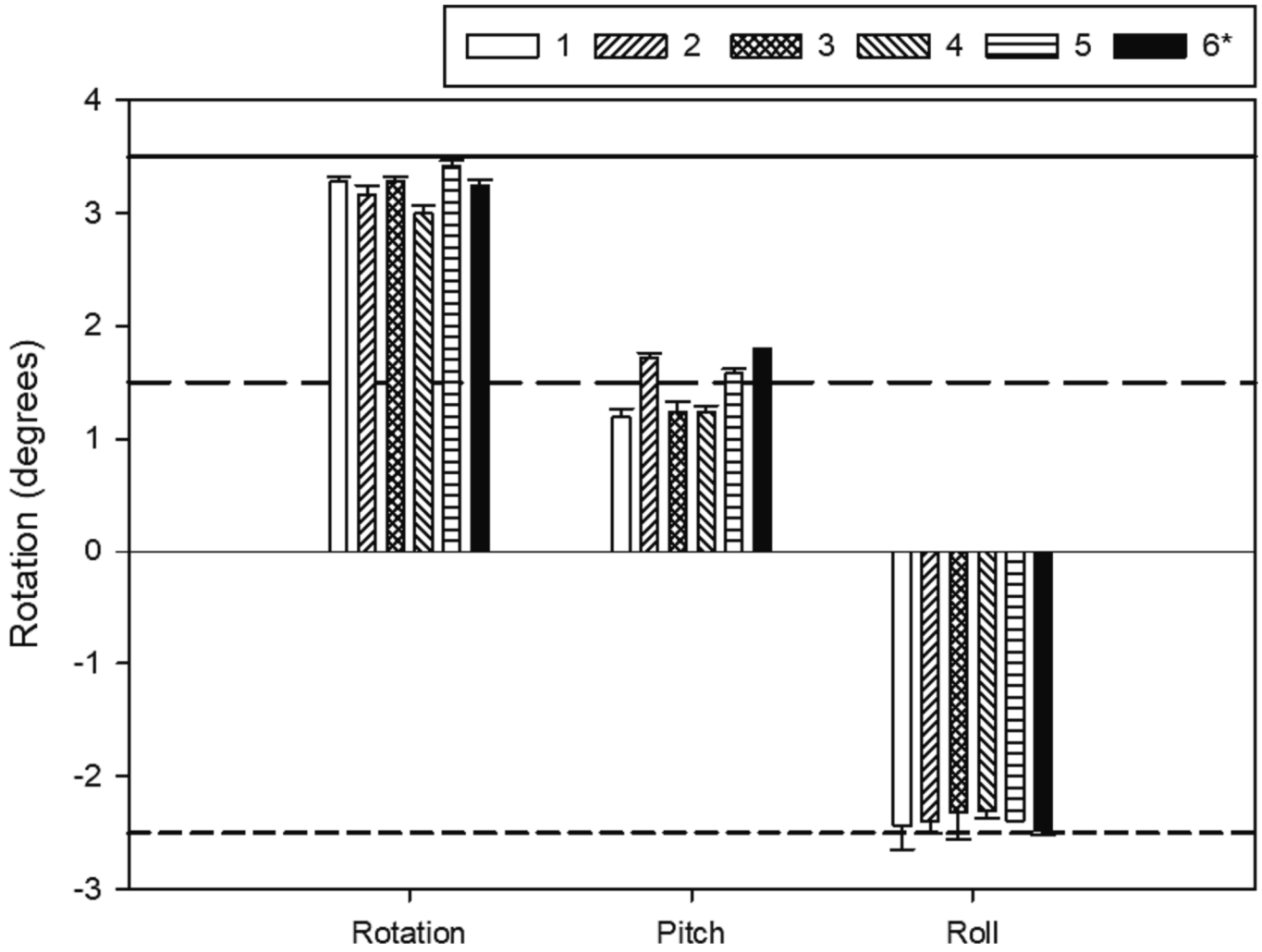

Fig. 5. Average rotational shifts across 5 measurements, for each phantom, corrected for 'actual' cube offsets obtained by CT-synthetic CT registration. Legend identifies centre and printer, as per Table 1, where * represents the additional PLA hybrid phantom produced by the NICC. Designed fabricated offset values of 3.5°, 1.5° and −2.5° in rotation, pitch and roll are given by the black solid, medium-dashed, and fine- dashed lines respectively.

different linac, whereby this study performed daily QA using only a single phantom on a single linac. However, registration was performed for the five independently produced PLA phantoms and a PLA hybrid phantom. For phantoms 1–5 the average rotational corrections were found to be 3.3 ± 0.2°, 1.3 ± 0.5° and −2.3 ± 0.3° in rot, pitch and roll with these corrections measured as 3.4 ± 0.1°, 1.8 ± 0.0° and −2.5 ± 0.1 on average for phantom 6*. This gave differences from the rotational offsets of −0.3 ± 0.2°, −0.2 ± 0.5° and 0.2 ± 0.3° in rot, pitch and roll respectively, for phantoms 1–5 and for the PLA hybrid these differences were −0.1 ± 0.1°, 0.3 ± 0.0° and 0.0 ± 0.1°. Similar to Woods et al, the 2σ uncertainty in these reported values approached or exceeded the AAPM rotational tolerance when combining the registration data for several independent phantoms. Woods et al concluded that given the increase in uncertainty, combined registration values should not be used as a baseline for QA, as tolerances may more likely be exceeded, which the combined registration values reported in this study also reflect. It is therefore recommended that baseline registration values are determined for each independent phantom, such that variations between phantoms is a product of their additive manufacture is negligible. If baseline values for phantom 6* are considered to be the average rotational corrections over the first three months, the differences between expected and observed corrections are much smaller than those observed when using the offset values as expected. Additionally, this study attempted to mitigate the effects of 3D-printing by accounting for the offsets that exist when registering CTs of each phantom to a rotation-free synthetic CT. Whilst this appears to reduce the variability found between phantoms, it should be considered that these 'actual' cube offsets measured may not be due to 3D-printing in isolation, where phantom setup errors may also have an impact on the observed 'actual' offsets. Further work could investigate the occurrence of 'actual' offsets and their origin by obtaining more than one CT image for each phantom, with varying slice thicknesses, or comparing CBCT images obtained on a treatment couch with a rotation-free synthetic CT, prior to rotational matching.

It should be noted that for phantom 6*, the observed correctional differences in pitch are much larger than in the other two rotational dimensions. This was not observed in the rotational corrections observed for phantoms 1–5. Phantom 6* was produced using a different method to phantoms 1–5 by printing the cube structures separately to the main body before inserting them to form the complete phantom, which may have impacted the orientation of the cubes when inserted. Additionally, of the three fabricated rotational offsets, pitch has the smallest value which may have resulted in pitch sifts from the initial setup being less-easy to observe than the other, larger, rotations resulting in less-certain image matching. This study investigated the clinical implementation of one phantom using one linac, future studies may involve the use of multiple treatment machines, where results could be obtained for multiple phantoms to evaluate individual couch performance. An additional consideration for future studies would be the

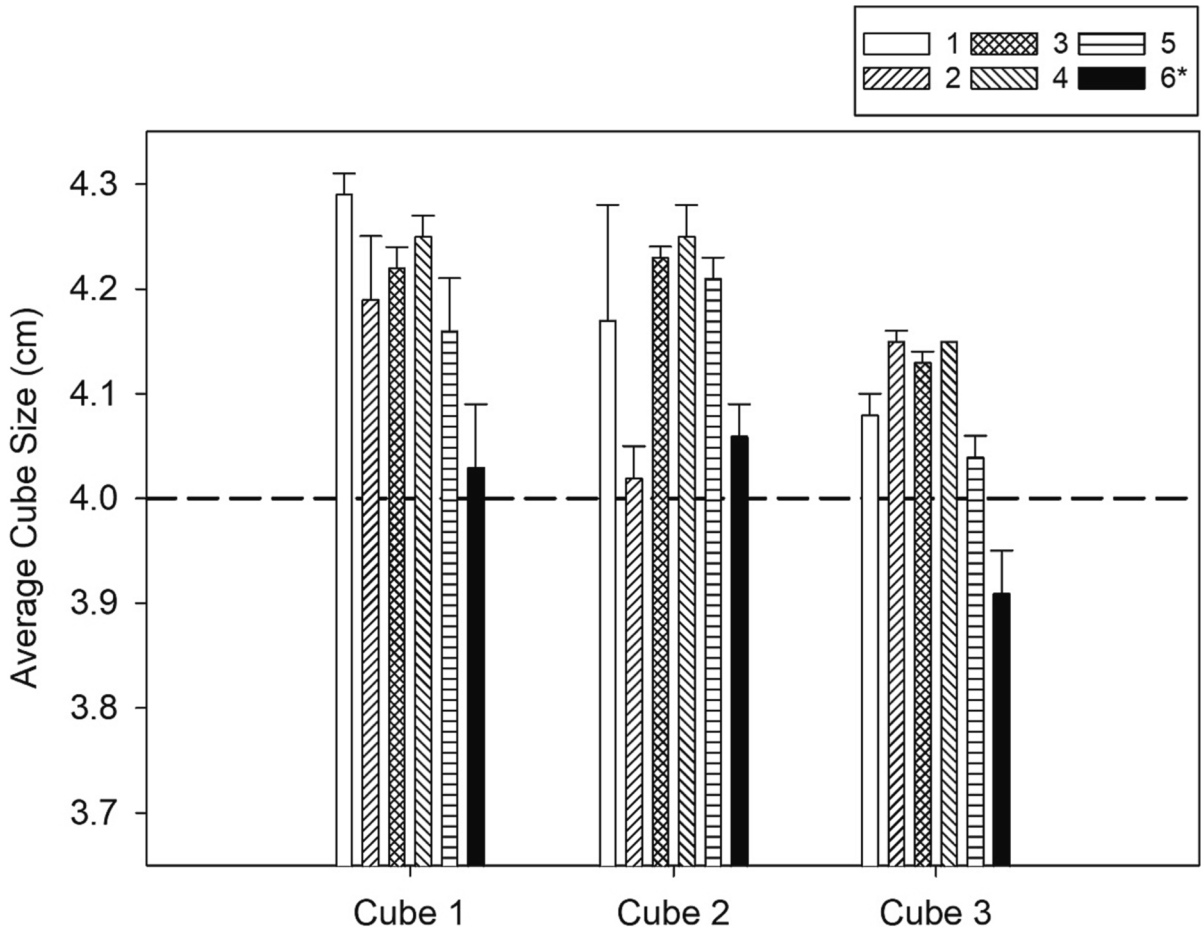

Fig. 6. The average size of each of three internal cube structures, where cubes 1,2,3 are identified in Fig. 1(b). Legend identifies both centre and printer used, as per Table 1, where * indicates the additional PLA hybrid phantom. Dashed horizontal line represents intended cube size.

implementation of tests involving smaller rotational angles, to evaluate the ability of the 6DoF couch in correcting smaller rotational offsets.

The reproducibility of phantom production, using fused deposition modelling, across multiple centres with different printers and material manufacturers was investigated by considering variations in geometry and HU. There was found to be no significant difference in average cube size between the five PLA phantoms, with a difference only becoming statistically significant when the cubes are fabricated using a hybrid thermoplastic. To measure the accuracy of 3D-printing in this study, the average cube sizes across each phantom were compared to the intended size of 4.00 cm in each dimension. Studies [16–17] investigating the dimensional accuracy of FDM printers to produce rapid prototyping models, have reported dimensional errors in the range 0.21–0.56 mm. In this study, the average dimensional difference of cube structures printed with PLA, compared to the designed size, was found to be 0.17 ± 0.04 cm. However, for the five PLA-only phantoms, each cube structure had two outer walls, and the region of the phantom body where the cube was to be located had two inner walls, all with thickness 0.4 mm, arising from the merging of two separate STL files. Phantoms 1–5, therefore, appeared to have larger internal cube structures, due to HU matching of inner layers of the hollow and outer layers of each cube, resulting in a 0.8 mm increase in the measured cube size along each dimension. However, the large difference between the HU of the StoneFil^{TM} cubes and the surrounding phantom body result in the inner layers of the hollow, which are printed with PLA, having negligible contribution to the measured cube size. Fig. 8 shows a profile across one of the cube structures for phantoms 5 and 6*, where a registration between CTs has been performed. It can be seen in Fig. 8, that the size values (in cm) corresponding to the half-maximum HU for PLA (phantom 5) are further from the expected value of ± 2 cm than those for cube structures printed with StoneFil^{TM} (phantom 6*).

The average HU determined for PLA, agrees with previous literature [18–21] where values have been reported in the range of 0–200. However, a statistically significant difference in measured HU was found between phantoms 1 and 2–5, with phantom 1 measuring HU much lower than expected. From a post-print questionnaire completed by each centre, it was found that this phantom was produced with a reduced flow rate (90%) of that in the initial STL file. Whilst one other centre also opted to reduce the flow rate to 90%, the nozzle used on the printer was larger in diameter, 0.5 mm. With a 0.4 mm nozzle and a reduced flow rate, phantom 1 may have experienced under-extrusion in comparison to the other four. Additionally, phantom 1 was produced with a higher print speed (60mms^{-1}) compared to phantoms 2–5 (30-45mms^{-1}). Which, in combination with the factors previously discussed, and contributions of other print settings, such as layer height, may have impacted the calculated HU in the volume of interest of the phantom, due to reduced density [22–24]. Furthermore, the quoted mass density by the PLA manufacturer of phantom 1 was slightly lower than that of phantoms 2–5 (Table 1) which may have contributed to the reduced HU observed. In this study, each centre printed with varying colours of PLA, where the colour pigment can affect measured HU as described by Fonseca et al [25], this may account for some of the variation in HU observed between phantoms 1–5. Fonseca et al additionally investigated the long-term stability of various 3D-printed materials. It was found that, whilst still stable, a PLA and stone hybrid material showed the largest variation in HU after 150 days. The effect of moisture absorption on certain materials over time, therefore, may impact the HU initially measured. The Hounsfield Units presented in this study are for regions

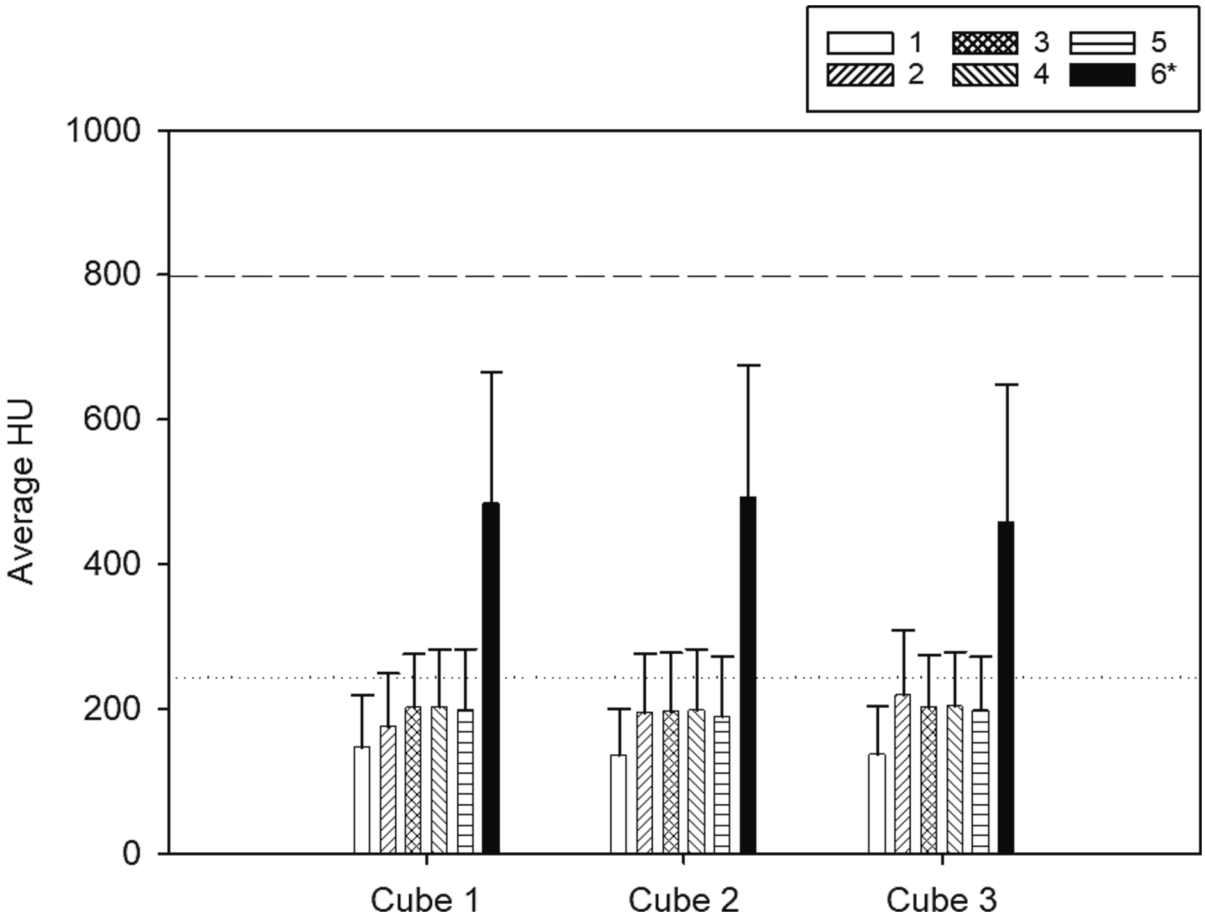

Fig. 7. The average HU of each of the cube structures, for each phantom, where cubes 1,2,3 are identified in Fig. 1(b). Legend identifies centre and printer, as per Table 1, where * represents the additional PLA hybrid phantom produced by the NICC. Dashed line and dotted line represent the expected HU of Stonefil and PLA, respectively based on calibration data.

printed with 100% infill density. Therefore, it is expected, as per the literature [26–29], that the associated uncertainties are at a minimum due to minimal presence of air gaps. A study by Madamesila et al [30] demonstrated the relationship between HU and infill density of 3D-printed samples, where High-Impact-Polystyrene (HIPS) samples with lower infill densities were shown to give rise to lower HU and larger uncertainties due to increasing presence of air within a specified region. Similarly, Kairn et al [31] demonstrated larger standard deviations in material properties for ABS samples printed with lower infill percentage. There was found to be no statistically significant difference between the measured differences in rotational corrections for each phantom, and differences in cube sizes or differences in HU. Therefore, despite small geometrical and radiological variations which arise as a factor of the 3D-printing process, these variations did not significantly impact the function of the phantom in performing rotational couch QA.

The use of a secondary thermoplastic in the study demonstrated the ease of personalisation of 3D-printed phantoms for a desired purpose, with greater CT contrast being achieved by the PLA hybrid phantom. However, the method of fabrication was more complex with the internal cube structures being printed independently to the main body. Using this method across multiple centres would have been more challenging, with a greater opportunity for geometrical variations to arise during fabrication. This production technique may have contributed to the statistically significant difference in average cube size between the multi-material phantom and those made utilising only PLA. To streamline the production of multi-material phantoms, centres with a capable printer could make use of dual extrusion [32], whereby the cubes would be printed with a second material alongside the main PLA body. This method of fabrication requires additional considerations as it requires the purchase of more than one printing filament, which may be a limitation for a centre for which purchase of a single, larger, spool of PLA would be more economically beneficial.

Limitations of this work include printing fails and defects, common to fused deposition modelling, which can affect the final print quality [33–34]. In this study, all but one centre experienced a printing fail requiring alteration of printing settings and repetition of a print. Each manufacturer of 3D-printable thermoplastic will have different production tolerances, which may affect the print quality if settings are not uniquely optimised. Centres should, therefore, establish quality control designed to optimise the printing settings for the specific material in use, prior to the commencement of a print, to mitigate negative effects on print quality induced by poor choice of settings. Commonly altered settings such as printing temperature, bed temperature, printing speed, flow rate and layer height can be optimised for unique printer-material combinations through the production of small test models, designed to probe change in settings. For example, printing a calibration model with regions printed at varying temperatures, encapsulating the range recommended by the manufacturer, can highlight the optimal print temperature for the specific printer in use, through visual observation of print finish. For each unique printer-material combination, a record of optimal settings could be kept, which can then be used as a base when printing with known materials to reduce the likelihood of the print quality being affected by poor setting choice. At the Northern Ireland Cancer Centre, work is currently being performed to establish a quality-system for 3D-printing. This includes the process of material calibration, as previously discussed, in addition to routine printer maintenance to

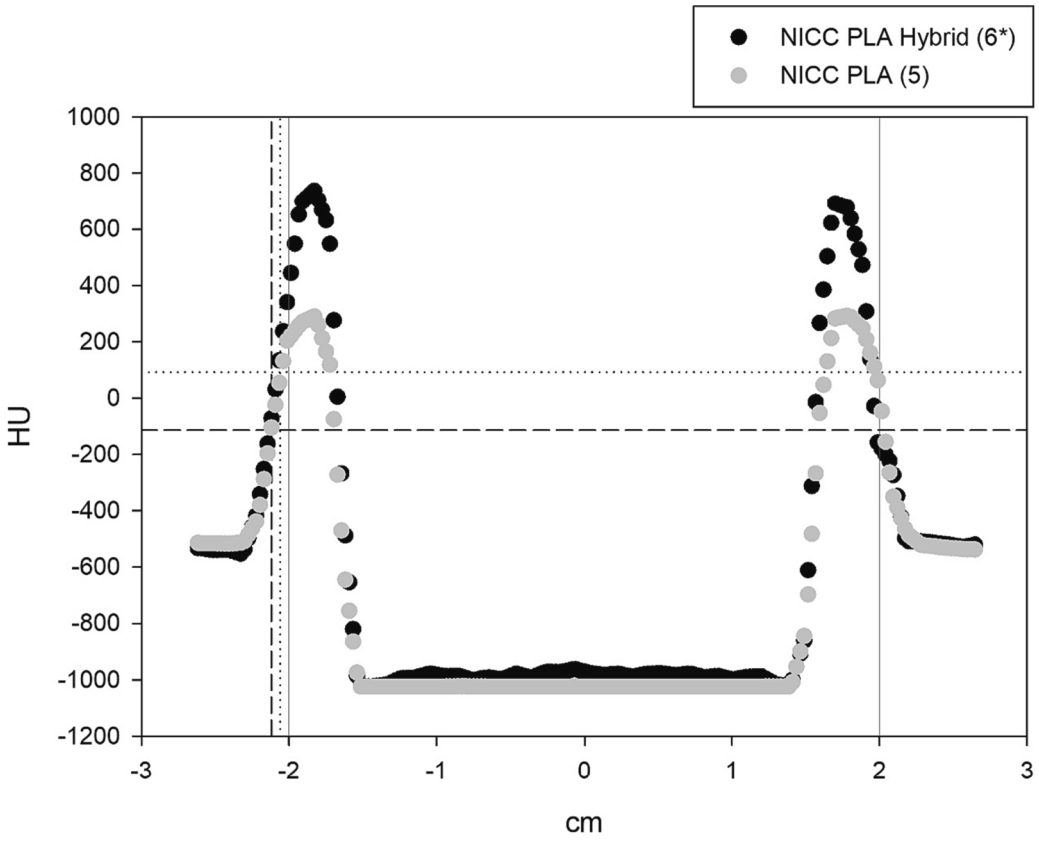

Fig. 8. Profile across one cube in one dimension in phantoms 5 and 6*. Solid lines at +/- 2 cm representing the intended size of the cube structures. Dotted and dashed lines demonstrate FWHM of phantoms 6* and 5 respectively, for the first peak.

ensure the printer is performing optimally. Additional measures to improve print quality such as pre-heating a printer's enclosure or the use of commercial adhesives should be considered [29]. A further limitation in the measurements obtained for cube geometry and HU would be the presence of partial volume effects, due to using 2 mm slice thickness. Whilst previous work performed at NICC confirmed negligible change in HU with altered slice thickness, the impact of partial volume effects on geometrical measurement should be considered, where 1 mm slice thickness would be recommended for future studies. Additionally, all imaging, which was used for determination of HU values, was performed on the same CT scanner, these HU values will therefore be dependent on the calibration curve for this CT scanner.

This study demonstrated the reproducibility of 3-dimensional printing across multiple centres, through the verification of minimal variation in geometry between prints. This method of phantom production, therefore, has the potential to be implemented in multi-centre audits whereby independent centres may make use of different 3D printers or material suppliers. Fuse deposition modelling, the 3D printing technique utilised in this work, has the benefit of utilising thermoplastics which are relatively inexpensive and can be used for an increasing number of applications. This could be of benefit in low- and middle-income countries, where the low production cost associated with additive manufacturing can be taken advantage of.

5. Conclusion

This study demonstrated the use of additive manufacturing to produce a novel QA phantom capable of sub-degree couch correction. All rotational corrections recorded over a 20-month period are within 0.5° of the fabricated rotational offsets, as per AAPM recommendation, demonstrating the potential for this phantom design to be implemented into a routine quality control program. This work also demonstrated the feasibility of printing across multiple centres from a single original file is possible, where suggestions to minimise inter-centre variations through the performance of 3D-printing quality assurance have been discussed.

Declaration of Competing Interest

The authors declare that they have no known competing financial interests or personal relationships that could have appeared to influence the work reported in this paper.

Acknowledgements

Catarina Veiga was supported by the Royal Academy of Engineering under the Research Fellowship scheme (RF\201718\17140). This work was supported in part by The Royal Society Research Grants (RGS/R2/202025).

This research was supported by funding from Friends of the Cancer Centre. The authors would like to extend thanks to those from ImSimQA™ who contributed to this study.

Appendix A. Supplementary data

Supplementary data to this article can be found online at https://doi.org/10.1016/j.ejmp.2023.103136.

References

[1] Yan D, Ziaja E, Jaffray D, Wong J, Brabbins D, Vicini F, et al. The Use of Adaptive Radiation Therapy to Reduce Setup Error: A Prospective Clinical Study. Int J Radiat Oncol 1998;41(3):715–20. https://doi.org/10.1016/s0360-3016(97)00567-1. PMID: 9635724.

[2] Klein Eric E, Hanley J, Bayouth J, Yin F-F, Simon W, Dresser S, et al. Task Group 142 report: Quality assurance of medical accelerators. Med Phys 2009;36:4197–212. https://doi.org/10.1118/1.3190392.

[3] Smith K, Balter P, Duhon J, White GA, Vassy DL, Miller RA, et al. AAPM medical physics practice guideline 8.a.: linear accelerator performance tests. J Appl Clin Med Phys 2017;18(4):23–39.

[4] Fu C, Ma C, Shang D, Qiu Q, Meng H, Duan J, et al. Geometric Accuracy Evaluation of a Six-Degree-of-Freedom (6-DoF) Couch with Cone Beam Computed Tomography (CBCT) Using a Phantom and Correlation Study of the Position Errors in Pelvic Tumor Radiotherapy. Transl Cancer Res 2020;9(10):6005–12.

[5] Cheon W, Cho J, Ahn SH, Han Y, Choi DH, et al. High-precision quality assurance of robotic couches with six degrees of freedom. Phys Med 2018;49:28–33. https://doi.org/10.1016/j.ejmp.2018.04.008.

[6] Dumas J-L, Fawzi M, Masset H, Losa S, Dal R, Pierrat N, et al. Independent 6D Quality Assurance of Stereotactic Radiotherapy Repositioning on Linacs. Cancer Radiother 2020;24(3):199–205.

[7] Zhou S, Li J, Du Y, Yu S, Wang M, Wu H, et al. Development and Longitudinal Analysis of Plan-Based Streamlined Quality Assurance on Multiple Positioning Guidance Systems With Single Phantom Setup. Front Oncol 2021;11:683733. https://doi.org/10.3389/fonc.2021.683733.

[8] Zhang Q, Driewer J, Wang S, Li S, Zhu X, Zheng D, et al. Accuracy evaluation of a six-degree-of-freedom couch using cone beam CT and IsoCal phantom with an in-house algorithm. Med Phys 2017;44(8):3888–98. https://doi.org/10.1002/mp.12342.

[9] Rance T, Yeo A, Leary M, Brandt M and Kron T.A systematic review on 3D-Printed imaging and dosimetry phantoms in radiation therapy. Technology in cancer research and Treatment, Vol 18, 1-14. doi: 10.1177/1533033819870208.

[10] McGarry C K, Grattan L J, Ivory A M, Leek F, Liney G P, Liu Y, et al., Tissue mimicking materials for imaging and therapy phantoms: a review. Phys Med Biol. 2020;65:23TR01 doi: 10.1088/1361-6560/abbd17.

[11] Woods K, Ayan AS, Woollard J, Gupta N. Quality Assurance for a Six Degrees-of-freedom Table Using a 3D Printed Phantom. J Appl Clin Med Phys 2017;19(1):115–24. https://doi.org/10.1002/acm2.12227.

[12] Popreeda T, Masa-nga W, Deeharing A, Udee N, Tannanonta C, Thongsawad S. Automating QA analysis for a six-degree-of-freedom (6DOF) couch using image displacement and an accelerometer sensor. Phys Med 2022;101:129–36. https://doi.org/10.1016/j.ejmp.2022.08.007.

[13] Giacometti V, King RB, McCreery C, Buchanan F, Jeevanandam P, Jain S, et al. 3D-printed patient-specific pelvis phantom for dosimetry measurements for prostate stereotactic radiotherapy with dominant intraprostatic lesion boost. Phys Med 2021;92:8–14.

[14] Okkalidis N, Bliznakova K, Kolev N. A filament 3D printing approach for CT-compatible bone tissues replication. Phys Med 2022;102:96–102. https://doi.org/10.1016/j.ejmp.2022.09.009.

[15] Patel I, Weston S, Palmer A. Physics Aspects of Quality Control in Radiotherapy. Institute of Physics and Engineering in Medicine 2018. -IPEM Report 81.

[16] Petropolis C, Kozan D, Sigurdson L. Accuracy of medical models made by consumer-grade fused deposition modelling printers. Plast Surg (Oakv) 2015;23(2):91–4. https://doi.org/10.4172/plastic-surgery.1000912.

[17] Maschio F, Pandya M, Olszewski R. Experimental Validation of Plastic Mandible Models Produced by a "Low-Cost" 3-Dimensional Fused Deposition Modeling Printer. Med Sci Monit 2016;22(22):943–57. https://doi.org/10.12659/msm.895656.

[18] Ma D, Gao R, Li M, Qiu J. Mechanical and medical imaging properties of 3D-printed materials as tissue equivalent materials. J Appl Clin Med Phys 2021;23(2):e13495.

[19] Oh SA, Kim MJ, Kang JS, Hwang HS, Kim YJ, Kim SH, et al. Feasibility of Fabricating Variable Density Phantoms Using 3D Printing for Quality Assurance (QA) in Radiotherapy. Progress in Medical Physics 2017;28(3):106.

[20] Park S-Y, Choi N, Choi BG, Lee DM, Jang NY. G, Lee D M and Jang N Y Radiological Characteristics of Materials Used in 3-Dimensional Printing with Various Infill Densities. Prog Med Phys 2019;30(4):155.

[21] Okkalidis N, Marinakis G. Technical Note: Accurate Replication of Soft and Bone Tissues with 3D Printing. Med Phys 2020;47(5):2206–11. https://doi.org/10.1002/mp.14100.

[22] Czyzewski P, Marciniak D, Nowinka B, Borowiak M, Bielinski M. Influence of Extruder's Nozzle Diameter on the Improvement of Functional Properties of 3D-Printed PLA Products. Polymers 2022;14:356. https://doi.org/10.3390/polym14020356.

[23] Triyono J, Sukanto H, Saputra RM, Smaradhana DF. The effect of nozzle hole diameter of 3D printing on porosity and tensile strength parts using polylactic acid material. Open Eng 2020;10:762–8. https://doi.org/10.1515/eng-2020-0083.

[24] Koutsouvelis N, Rouzaud M, Dubouloz A, Nouet P, Jaccard M, Garibotto V, et al. 3D printing for dosimetric optimization and quality assurance in small animal irradiations using megavoltage X-rays. Z Med Phys 2020;30(3):227–35.

[25] Fonseca P G, Rezaeifar B, Lackner N, Haanen B, Reniers B and Verhaegen F, Dual-energy CT evaluation of 3D printed materials for radiotherapy applications. Phys Med Biol. 2023; 68:035005 doi: 10.1088/1361-6560/acaf4a.

[26] Talalwa L, Natour G, Bauer A, Drzezga A, Beer S. Radiological characteristics of a new experimental rubber elastomeric polymer used in 3-dimensional printing with different infill densities and patterns. J Phys Commun 2020;4:125006. https://doi.org/10.1088/2399-6528/abd1c3.

[27] Andrade MAB, Fin APC, Alves CDO, Soares FAP, Savi MBMB, Potiens MDPA. Visual impact of infill percentages in visual homogeneity for 3D printed imaging phantoms. Brazilian J Radiat Sci 2020;08–01A:01–10. https://doi.org/10.15392/bjrs.v8i1A.919.

[28] Özsoykal I, Husemoglu R B and Yurt A, Radiological Evaluation of The Effects of Printing Parameters on 3D-Printed Cylindrical LW-PLA Samples: preliminary Results. J Med Innov Technol. 2021; 3(2): 28-34 doi: 10.51934/jomit.1037540.

[29] Choi Y, Jang YJ, Kim KB, Bahng J, Choi SH. Characterization of Tissue Equivalent Materials Using 3D Printing for Patient-Specific DQA in Radiation Therapy. Appl Sci 2022;12:9768. https://doi.org/10.3390/app12199768.

[30] Madamesila J, McGeachy P, Barajas JEV, Khan R. Characterizing 3D printing in the fabrication of variable density phantoms for quality assurance of radiotherapy. Phys Med 2019;32:242–7. https://doi.org/10.1016/j.ejmp.2015.09.013.

[31] Kairn T, Crowe S.B and Markwell T. Use of 3D Printed Materials as Tissue-Equivalent Phantoms. Springer International Publishing Switzerland. World Congress on Medical Physics and Biomedical Engineering, June 7-12 2015, Toronto Canada. IFMBE Proceedings 51 DOI: 10.1007/978-3-319-19387-8_179.

[32] Vaezi M, Chianrabutra S, Mellor B, Yang S. Multiple Material Additive Manufacturing – Part 1: A Review. Virtual Phys Prototyping 2013;8(1):19–50. https://doi.org/10.1080/17452759.2013.778175.

[33] Gordeev EG, Galushko AS, Ananikov VP, Improvement of quality of 3D-printed objects by elimination of microscopic structural defects in fused deposition modeling. Plos One. 2018; 13(6): e0198370 doi: 10.1371/journal.pone.0198370.

[34] Baechle-Clayton M, Loos E, Taheri M, Taheri H. Failures and Flaws in Fused Deposition Modelling (FDM) Additively Manufactured Polymers and Composites. J Compos Sci 2022;6(7):202. https://doi.org/10.3390/jcs6070202.